Earth and Planetary Science Letters, 85 (1987) 91–104
Elsevier Science Publishers B.V., Amsterdam – Printed in The Netherlands

[1]

The Pan-African continental margin in northeastern Africa: evidence from a geochronological study of granulites at Sabaloka, Sudan

A. Kröner [1], R.J. Stern [2], A.S. Dawoud [3], W. Compston [4] and T. Reischmann [5]

[1] *Institut für Geowissenschaften, Universität Mainz, Postfach 3980, 6500 Mainz (F.R.G.)*
[2] *Center of Lithospheric Studies, University of Texas at Dallas, P.O. Box 688, Richardson, TX 75083-0688 (U.S.A.)*
[3] *Department of Geology, University of Khartoum, P.O. Box 321, Khartoum (Sudan)*
[4] *Research School of Earth Sciences, Australian National University, G.P.O. Box 4, Canberra, ACT 2601 (Australia)*
[5] *Max-Planck-Institut für Chemie, Postfach 3060, 6500 Mainz (F.R.G.)*

Received February 17, 1987; revised version accepted June 5, 1987

Ion microprobe zircon ages, a Nd model age and Rb-Sr whole-rock dates are reported from the high-grade gneiss terrain at Sabaloka on the River Nile north of Khartoum, formally considered to be part of the Archaean/early Proterozoic Nile craton. The granulites, which are of both sedimentary and igneous derivation, occur as remnants in migmatites. Detrital zircon ages range from ≈ 1000 to ≈ 2650 Ma and prove the existence of Archaean to late Proterozoic continental crust in the sedimentary source region. The Nd model age for one sedimentary granulite is between 1.26 (T_{CHUR}) and 1.70 (T_{DM}) Ga and provides a mean crustal residence age for the sedimentary precursor. Igneous zircons in enderbitic gneiss crystallized at 719 ± 81 Ma ago, an age that also corresponds to severe Pb loss in the detrital zircons and which probably reflects the granulite event at Sabaloka. The Rb-Sr data indicate isotopic homogenization at about 700 Ma ago in the granulites and severe post-granulite disturbance at ≈ 570 Ma in the migmatites. We associate this disturbance with hydration, retrograde metamorphism and anatexis that produced undeformed granites ≈ 540 Ma ago. The ≈ 700 Ma granulite event at Sabaloka suggests that this part of the Sudan belongs to the Pan-African Mozambique belt while the ancient Nile craton lay farther west. The gneisses studied here may represent the infrastructure of the ancient African continental margin onto which the juvenile arc assemblage of the Arabian-Nubian shield was accreted during intense horizontal shortening and crustal interstacking of a major collision event.

1. Introduction

Extensive areas of medium- to high-grade Precambrian gneisses occur in southern and north-central Sudan and in the neighbouring territories of Ethiopia, Chad, Libya and Egypt [1]. These rocks have been identified with an ancient cratonic complex, variously named the Nile craton [2], the Sudan shield [1] and the East Sahara craton [3] and are considered to be considerably older than the adjacent Nubian shield of Pan-African ($\approx$ 500–950 Ma) age [3–6]. The relationship between this cratonic domain, typified by the ≈ 2.6 Ga old granulites and gneisses at Ouweinat [7] (Fig. 1), and the accretionary juvenile arc terrain east of the River Nile [8] is central to the understanding of crustal growth processes during the Precambrian. It is therefore of considerable interest to identify the ancient continental margin in northeastern Africa and to portray its evolution in Pan-African times.

Field evidence to suggest that the low-grade metasediments and metavolcanics of the Pan-African association in Sudan overlie the higher-grade gneisses unconformably [5,6] was contradicted by Rb-Sr dating in the Bayuda Desert that showed the gneisses there to be of Pan-African age and that these rocks could not have been derived from crust older than ≈ 1000 Ma [9]. Archaean ages on granulites from the West Nile Complex of northern Uganda and the Oasis Ouweinat at the Egyptian/Libyan/Sudanese border as well as petrographic and structural similarities between these rocks and the granulitic "grey gneisses" of north-central Sudan led to the conclusion that there may have been a continuous

0012-821X/87/$03.50

Archaean crustal segment in the region, of which the Sabaloka granulites were part [5]. Vail [6], on the other hand, considered that the mid-Proterozoic West African craton extended across the continent into northeast Africa. It was emphasized that the Sudan gneisses do not form part of the

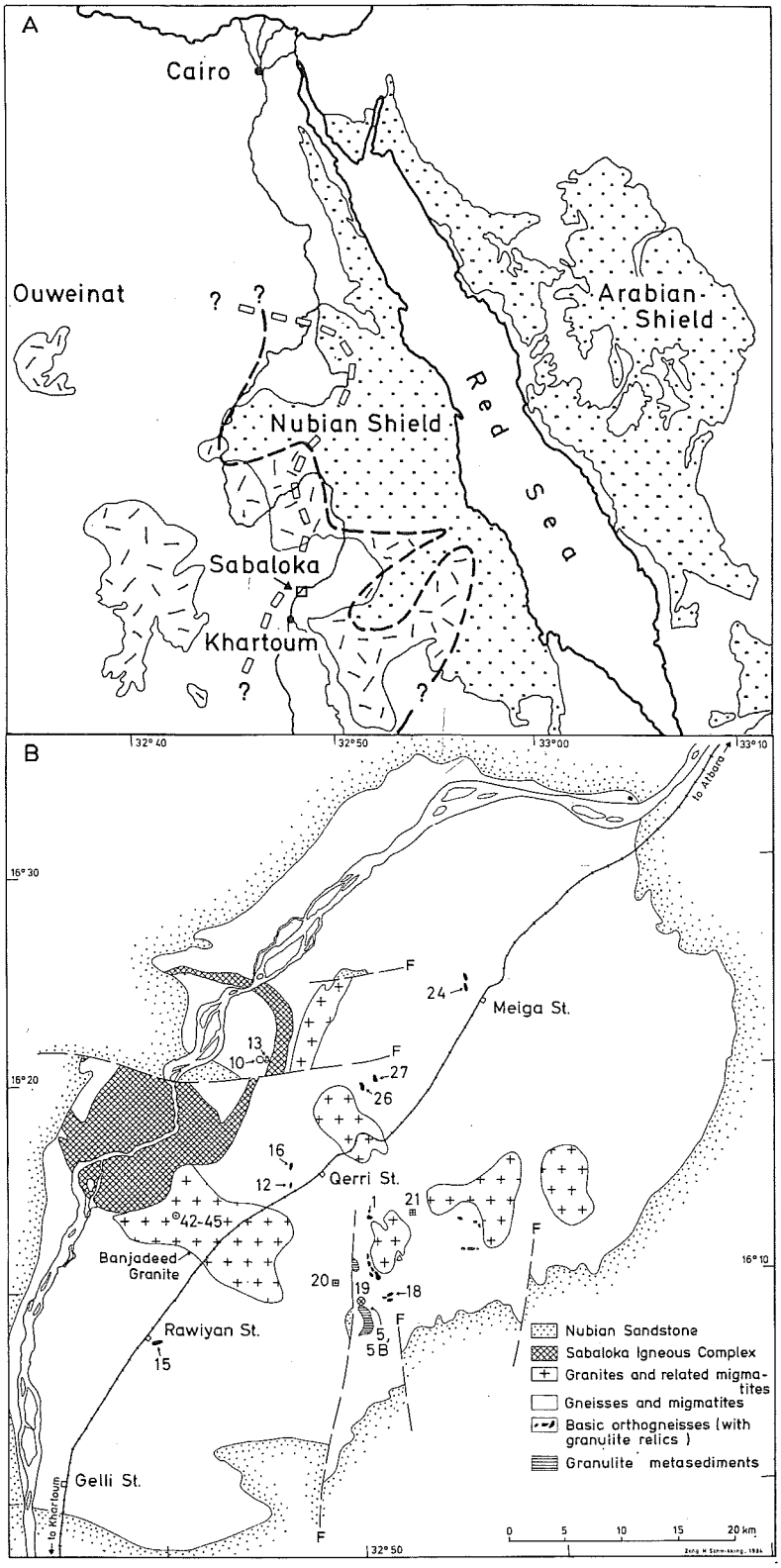

Fig. 1. A. Simplified map of northeastern Africa and Arabia showing approximate boundary between Pan-African "greenschist assemblage" (stippled) higher-grade gneisses of presumed pre-Pan-African age (hachured) [1] and interpreted as a presumed continental margin of the ancient Sudan shield [6]. Also shown is proposed continental margin [38] (open rectangles). B. Simplified geological map of Sabaloka area showing distribution of major rock units and sample locations.

broad Pan-African Mozambique belt that extends from Mozambique to Ethiopia along the east coast of Africa [10].

Using the ion-microprobe SHRIMP at the Australian National University and conventional Rb-Sr whole-rock geochronology we have dated granulites of igneous and sedimentary origin and their zircons as well as migmatites that probably represent retrogressed granulites and a granite from the grey gneiss terrain at Sabaloka, some 80 km north of Khartoum (Fig. 1). These rocks have previously been mapped [11] and studied petrographically [5] and consist of high-grade semipelitic to calcareous metasediments and interbanded charnockitic to enderbitic gneisses of presumed magmatic origin. The structural history is complex and reveals several phases of superposed folding [11], and we interpret the presently observed lithological banding as reflecting transposed sedimentary or igneous layering. Quantitative *P-T* determinations derived from microprobe analyses of mineral assemblages that equilibrated during the peak of metamorphism, indicate $T = 600–800\,^{\circ}C$ and $P = 6–8$ kbar, depending on the thermometer and barometer used (Dawoud, unpublished data). This suggests a crustal depth of 20–30 km for granulite formation. Gravity data indicate a present thickness of ≈ 40 km for the crust at Sabaloka [12].

The granulites occur as dark patches or discrete bands that range in size from a few centimetres to hundreds of metres within lower-grade biotite gneisses and migmatites (grey gneiss assemblage) and locally show evidence of slight retrogression [5]. The bulk of the grey gneisses are interpreted as retrograded granulites, produced during an influx of water into a dry and still hot assemblage [5]. Anatectic phenomena in the migmatites are widespread, and it can be shown in the field from contacts gradational between migmatites and granites that the coarse-grained, post-tectonic, red porphyritic granite plutons of the region are probably derived from such anatectic melts. We have investigated one of these plutons, the Banjadeed granite (Fig. 1), in order to date this granite-forming event. Sample localities are shown in Fig. 1.

2. Geochemistry

In order to interpret the significance of the isotopic data it is necessary to understand the nature of the granulites' protoliths. Major element and CIPW norm data for samples dated in this study are listed in Table 1. These data indicate that the granulites can be subdivided into two distinct groups. Group 1 is mafic to intermediate in composition (44–61% SiO_2, 2.7–6.7% MgO) and has relatively low K contents (0.07–1.63% K_2O). With the exception of the two felsic samples SAB 15 and 18, this group is also unusually calcic, with 19–26% CaO. The norms of this group therefore include very calcic plagioclase, abundant diopside and, commonly, wollastonite. These rocks are approximately saturated in silica and contain no normative corundum. Group 2 consists of three samples (SAB 5, 5B and 13) that are relatively siliceous (56–74% SiO_2) and contain comparatively litte calcium (1.0–1.7% CaO). The norms of this group include intermediate plagioclase compositions, significant amounts of corundum and hypersthene and abundant quartz. These rocks contain no normative diopside.

The nature of the premetamorphic precursors for group 1 is not easy to determine from geochemical data alone. The two felsic samples SAB 15 and 18 have major and trace element compositions similar to granodiorite, and the REE pattern of SAB 16 (Fig. 2) is also typical of granodiorite. Furthermore, SAB 18 has characteristic euhedral igneous zircons without evidence of sedimentary transport (Fig. 5). The high CaO content of the remaining 6 samples suggests them to be derived

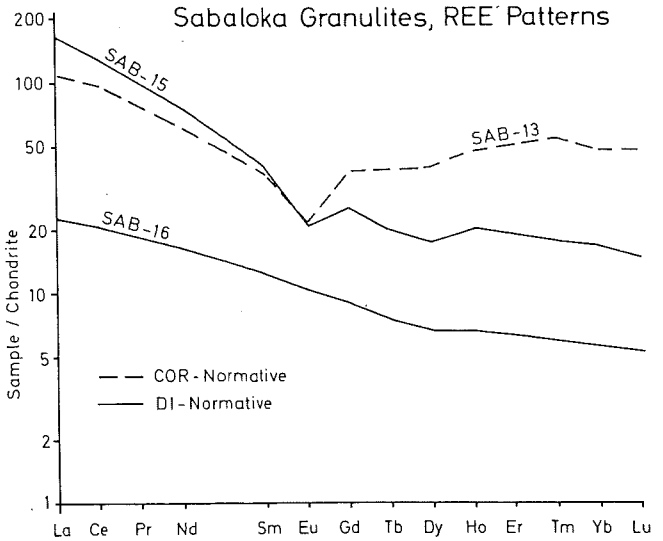

Fig. 2. Chondrite-normalized REE patterns for three Sabaloka granulites. For analytical data see Table 2.

TABLE 1

Major element and CIPW Norm data for Sabaloka granulites

	Diopside-normative								Corundum-normative		
	SAB 1*	SAB 12	SAB 15	SAB 16	SAB 18	SAB 24*	SAB 26*	SAB 27*	SAB 5	SAB 5B	SAB 13
Oxides (wt.%)											
SiO_2	47.34	43.65	58.85	46.52	61.07	47.32	46.50	50.10	72.00	73.83	55.45
TiO_2	0.59	0.49	0.87	0.58	0.65	0.61	0.53	0.52	0.90	0.49	1.32
Al_2O_3	12.45	16.49	16.96	14.04	16.76	12.72	11.30	12.80	12.51	12.93	21.57
Fe_2O_3	2.21	3.28	1.44	2.65	1.23	3.53	2.37	2.60	0.98	1.37	1.68
FeO	6.07	3.57	5.29	4.61	4.79	5.18	5.40	6.22	4.78	1.91	9.90
MnO	0.25	0.20	0.12	0.18	0.12	0.21	0.26	0.28	0.09	0.05	0.34
MgO	5.75	4.43	2.92	8.33	2.69	5.60	6.73	5.13	2.61	1.33	4.64
CaO	22.63	25.60	6.25	20.80	6.46	23.06	23.50	19.20	1.01	1.23	1.73
Na_2O	0.74	0.33	4.42	0.50	4.15	0.47	0.51	1.47	1.50	2.33	1.48
K_2O	0.07	0.21	1.63	0.44	1.36	0.42	0.25	0.71	2.25	3.67	0.74
P_2O_5	0.18	0.14	0.28	0.14	0.32	0.25	0.05	0.14	0.05	0.06	0.05
LOI	1.18	1.15	0.31	0.64	0.16	1.50	1.90	1.70	0.79	0.51	0.57
Total	99.46	99.54	99.34	99.43	100.29	100.87	99.36	100.77	99.47	99.71	99.47
Norms											
Ap	0.43	0.33	0.66	0.33	0.76	0.59	0.12	0.33	0.12	0.14	0.12
Il	1.12	0.93	1.65	1.10	1.23	1.16	1.01	0.99	1.71	0.93	2.51
Mt	3.20	4.76	2.09	3.84	1.78	5.12	3.44	3.77	1.42	1.99	2.44
Or	0.41	–	9.63	0.22	8.04	2.48	1.31	4.20	13.30	21.69	4.37
Plag	35.87	42.89	59.02	34.77	58.20	35.33	27.81	38.67	17.38	25.43	20.78
Ne	0.45	1.51	–	2.29	–	–	2.34	–	–	–	–
Cor	–	–	–	–	–	–	–	–	5.89	3.03	15.31
Qtz	–	–	8.25	–	13.11	0.78	–	1.08	45.72	41.03	26.58
Di	47.46	30.21	6.25	53.86	5.69	41.33	50.38	44.36	–	–	–
Wo	9.35	10.56	–	–	–	12.59	10.88	5.79	–	–	–
Hy	–	–	11.49	–	10.81	–	–	–	13.15	4.97	26.80
Lc	–	0.97	–	1.87	–	–	0.13	–	–	–	–
Cs	–	6.24	–	–	–	–	–	–	–	–	–
Normative plag. comp.	An_{85}	An_{100}	An_{37}	An_{100}	An_{40}	An_{89}	An_{100}	An_{68}	An_{27}	An_{22}	An_{40}

Analyses by conventional wet chemistry, University of Mainz; analyst: Th. Kost. Those marked with * are by plasma spectrometry; analyst: B. Zimanowski.

from anorthosites, and we interpret the fine layering in these rocks as relict igneous banding. An anorthositic origin is also supported by high Cr and Ni contents that are characteristic of mafic or ultramafic igneous rocks with light REE enrichment as shown in sample SAB 16 (Fig. 2). We suggest that our samples come from a lower crustal igneous complex similar to those reported from other Precambrian granulite terrains such as West Greenland [13] and the Limpopo mobile belt of southern Africa [14].

The premetamorphic precursor for group 2 was clearly sedimentary. These are well-layered rocks with well-rounded, detrital zircons (Fig. 3), and their major element composition with high SiO_2 and K_2O suggests that they were originally arkosic wackes (SAB 13) and siliceous arkoses or shales (SAB 5, 5B). Sample SAB 13 has an unusual REE pattern in being elevated in HREE and LREE (60–100 × chondrite) and having relatively little of the middle REE (40–40 × chondrite, exclusive of Eu). This may have resulted from mixing LREE-enriched lithic fragments with zircon or other detrital heavy minerals which preferentially incorporate the HREE into their lattices. Both the zircon and Rb-Sr data as well as a Nd model age presented below indicate that these metasediments were derived from older continental crust, a con-

TABLE 2

Trace element data (in ppm) for Sabaloka granulites

Element	SAB 1	SAB 12	SAB 15	SAB 16	SAB 18	SAB 24	SAB 26	SAB 27	SAB 5	SAB 5B	SAB 13
Cr	978	341	9	1137	33	826	1054	481	105	51	185
Ni	238	59	9	372	16	234	415	112	49	28	9
Cu	4.1	1.3	19	7.6	1.4	4.6	<1	<1	<1	7.3	50
Zn	136	78	89	61	96	114	247	217	137	60	200
Y	21	11	34	14	20	11	8.2	25	47	41	22
Zr	89	30	186	44	154	85	38	74	182	155	2.5
Nb	5.7	3.2	10	4.8	6.2	11	8.2	6.3	14	11	22
V	187	166	128	162	110	232	112	153	123	61	235
Co	55	51	37	60	54	56	53	41	103	74	77
Sc			17 *	28 *							40 *
Ba			485 *	81 *							362 *
U			3.3*	0.6*							1.5*
Th			8.8*	1.6*							8.7*
La			50.8*	7.15*							33.9*
Ce			105 *	16.8*							76.5*
Pr											9.3*
Nd			44.7*	9.7*							35.8*
Sm			7.52*	2.36*							6.89*
Eu			1.50*	0.75*							1.58*
Gd			6.5*	2.3*							9.8*
Tb			0.93*	0.35*							1.81*
Dy			5.65*	2.16*							12.9*
Ho			1.24*	0.46*							3.27*
Tm											1.59
Yb			3.25*	1.15*							9.91*
Lu			0.48*	0.166*							1.49*

Data by XRF, University of Mainz, those marked with * are data by instrumental neutron activation analysis, Max-Planck-Institut für Chemie, Mainz, Analyst: B. Spettel.

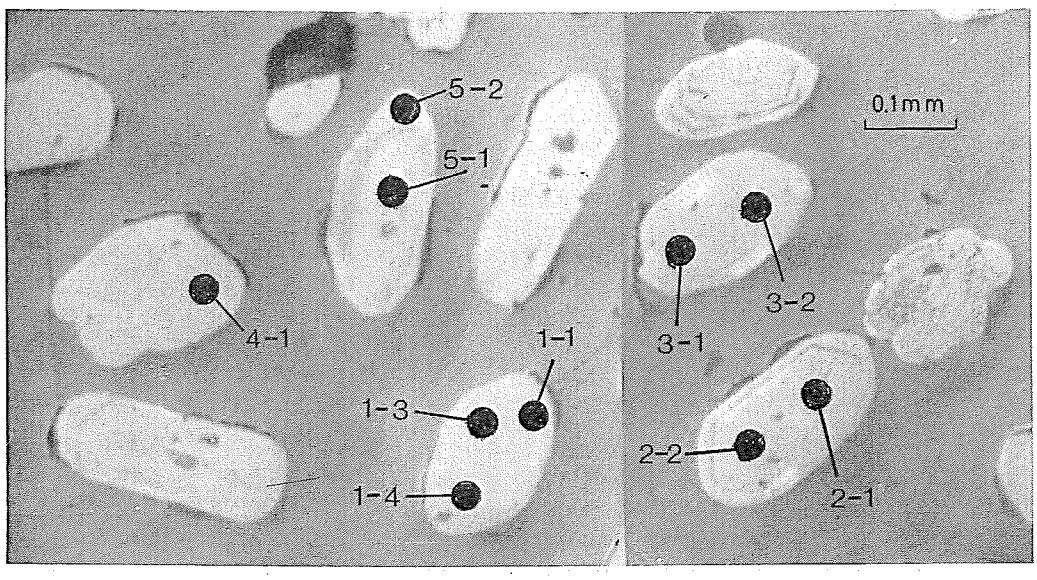

Fig. 3. Microphotograph in reflected light of sectioned and polished zircon grains from metasedimentary granulite sample SAB 5. Note core and rim in grain 5. Analyzed spots indicated in black. Numbers refer to analyses in Table 3.

clusion that is consistent with these originally having been mature terrigeneous deposits.

3. Geochronology

Zircons were separated by conventional concentration techniques and handpicking in 4 samples of the granulites (SAB 5, 5B, 12 and 18) and were mounted in separate fractions on an epoxy resin disk. The disk was then polished so that most grains were approximately sectioned in half, exposing their cores, and were analyzed on the SHRIMP ion microprobe [15]. U-Th-Pb analyses were performed using positive secondary ions sputtered from a 30–35 μm spot on the surface of the sectioned zircons by a 10 kV primary beam of negative oxygen ions. Mass resolution was 6500, at which all significant isobaric molecular interferences were separated from Pb^+, U^+, ThO^+ and UO^+ ions. Sensitivity for Pb isotopes was between 12 and 26 cps/ppm.

Since there is no significant mass fractionation of sputtered Pb^+ ions [16], $^{207}Pb/^{206}Pb$ ages could be determined directly from the observed $^{207}Pb^+/$

TABLE 3

Ion microprobe analyses of zircons from sample SAB, Sudan

Sample	Grain area	U (ppm)	Th (ppm)	Common ^{206}Pb (%)	$\frac{^{207}Pb}{^{206}Pb}$	$\frac{^{206}Pb}{^{238}U}$	$\frac{^{207}Pb}{^{235}U}$	$\frac{^{208}Pb}{^{232}Th}$	Ages (Ma) 208/232	206/238	207/206
SAB 5	1-1	516	627	1.6	0.1761± 15	0.4658±84	11.31 ±23	0.1377± 28	2607	2465	2617± 14
	1-3	499	265	0.6	0.1663± 13	0.3896±70	8.93 ±18	0.1440± 32	2720	2121	2521± 13
	1-4	699	1045	0.3	0.1769± 11	0.4639±83	11.31 ±22	0.1351± 26	2561	2457	2624± 10
	2-1	286	170	6.6	0.0711± 59	0.1471±28	1.44 ±12	0.0472± 35	932	885	959±170
	2-2	291	240	6.4	0.0734± 60	0.1624±31	1.64 ±14	0.0477± 29	941	970	1024±165
	3-1	636	862	1.0	0.1251± 16	0.330 ±59	5.53 ±13	0.1017± 21	1958	1838	1978± 23
	3-2	895	916	1.0	0.1189± 14	0.3179±57	5.21 ±12	0.0981± 20	1892	1780	1939± 21
	4-1	308	119	4.1	0.1086± 37	0.2627±48	3.93 ±16	0.0846± 56	1641	1503	1776± 62
	5-1	880	2040	1.9	0.1198± 15	0.3196±57	5.28 ±12	0.0660± 13	1292	1788	1953± 22
	5-2	1404	12	4.5	0.0908± 28	0.1564±28	1.96 ± 7	0.204 ±110	–	937	1442± 59
	6-1	262	80	4.1	0.1055± 56	0.2326±44	3.38 ±20	0.0750± 94	1461	1348	1724± 98
	7-1	383	241	5.5	0.0749± 44	0.1615±30	1.67 ±11	0.0475± 27	938	965	1065±118
	8-1	307	146	5.9	0.0730± 68	0.1599±31	1.61 ±16	0.0469± 53	926	956	1015±190
	9-1	404	49	6.0	0.0655± 60	0.1242±23	1.12 ±11	0.0326±142	649	755	792±195
	10-1	5797	10	0.1	0.0617± 4	0.1130±20	0.961±19	1.50 ± 6	–	690	663± 13
	11-1	473	97	3.5	0.0703± 36	0.1456±26	1.4 ± 8	0.0376± 56	746	876	937±105
	11-2	1911	260	1.4	0.0717± 9	0.1526±27	1.51 ± 3	0.0491± 22	969	915	976± 25
SAB 13	12-1	562	153	2.4	0.0691± 26	0.1475±26	1.41 ± 6	0.0473± 32	934	887	901± 78
	12-2	632	202	2.1	0.0712± 24	0.1579±28	1.55 ± 6	0.0493± 28	972	945	963± 69
SAB 5B	13-1	1790	7	2.0	0.0620± 13	0.1134±20	0.969±28	0.121 ± 84	2300	693	673± 45
	14-1	867	447	0.9	0.1229± 12	0.2895±51	4.90 ±10	0.0809± 20	1573	1639	1998± 17
	14-2	1035	8	1.7	0.0799± 27	0.1089±19	1.20 ± 5	0.651 ± 85	–	666	1194± 67
	15-1	294	109	5.4	0.0748± 59	0.1717±33	1.77 ±15	0.0506± 55	997	1022	1063±159
	16-1	883	251	2.3	0.0715± 19	0.1599±28	1.57 ± 5	0.0435± 24	861	956	971± 54
	17-1	252	84	13.0	0.0685±103	0.1363±29	1.29 ±20	0.0445± 97	880	824	884±315
	18-1	3386	9	0.3	0.0640± 7	0.1105±19	0.976±21	0.269 ± 59	–	676	745± 23
	19-1	732	613	0.5	0.1306± 9	0.3780±67	6.81 ±14	0.1148± 22	2196	2067	2106± 12
SAB 18	20-1	285	130	4.1	0.0607± 25	0.0901±16	0.754±35	–	–	556	627± 88
	21-1	232	124	5.5	0.0646± 30	0.0953±17	0.849±44	–	–	587	764± 98
	22-1	274	117	5.2	0.0661± 24	0.0980±17	0.892±38	–	–	602	809± 76
	23-1	266	114	4.7	0.0686± 27	0.0959±17	0.907±41	–	–	590	656± 81
	24-1	308	136	5.5	0.0630± 31	0.0939±17	0.816±44	–	–	579	708±105
	25-1	229	118	6.7	0.0653± 35	0.0930±17	0.838±49	–	–	573	786±113

Radiogenic Pb corrected for non-radiogenic Pb using the observed ^{204}Pb (SAB 5, 5B and 13), or using ^{208}Pb (SAB 18).

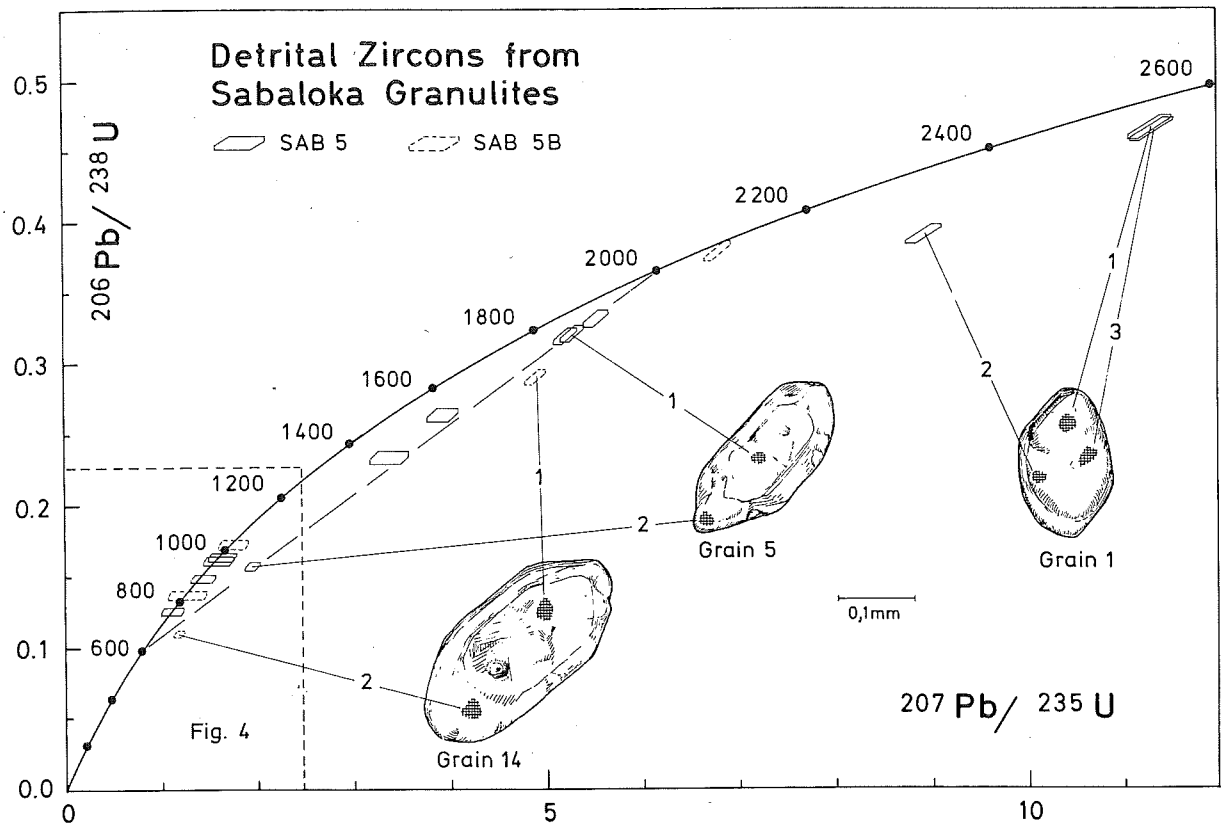

Fig. 4. Concordia diagram showing zircon data for granulites of sedimentary origin. Data boxes for each spot analysis are defined by standard errors in $^{207}Pb/^{206}Pb$, $^{207}Pb/^{235}U$ and $^{206}Pb/^{238}U$. Insets show sectioned grains as observed on polished epoxy disk and analyzed spots.

$^{206}Pb^+$ ratios, after correction for common Pb that is based on the measured $^{204}Pb^+/^{206}Pb^+$ ratio and a modelled common Pb composition [17] at the inferred age of each grain. For sample SAB 18 the errors in ^{204}Pb-corrected isotopic ratios were unusually large due to low ^{206}Pb, and for these data the common Pb content was calculated from the measured $^{208}Pb^+/^{206}Pb^+$ ratio and the radiogenic

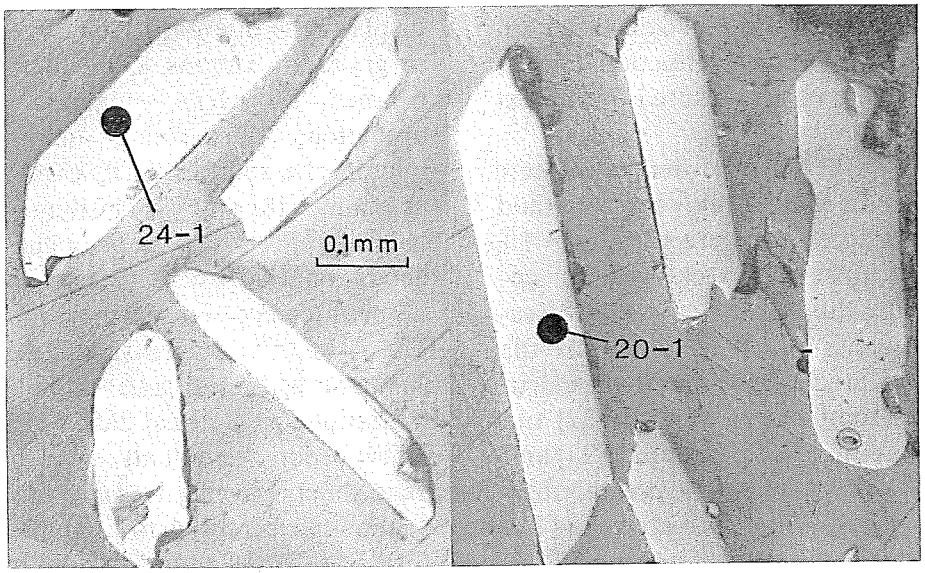

Fig. 5. Microphotograph in reflected light of sectioned and polished zircon grains from igneous granulite sample SAB 18. Analyzed spots in black and numbers refer to analyses in Table 3.

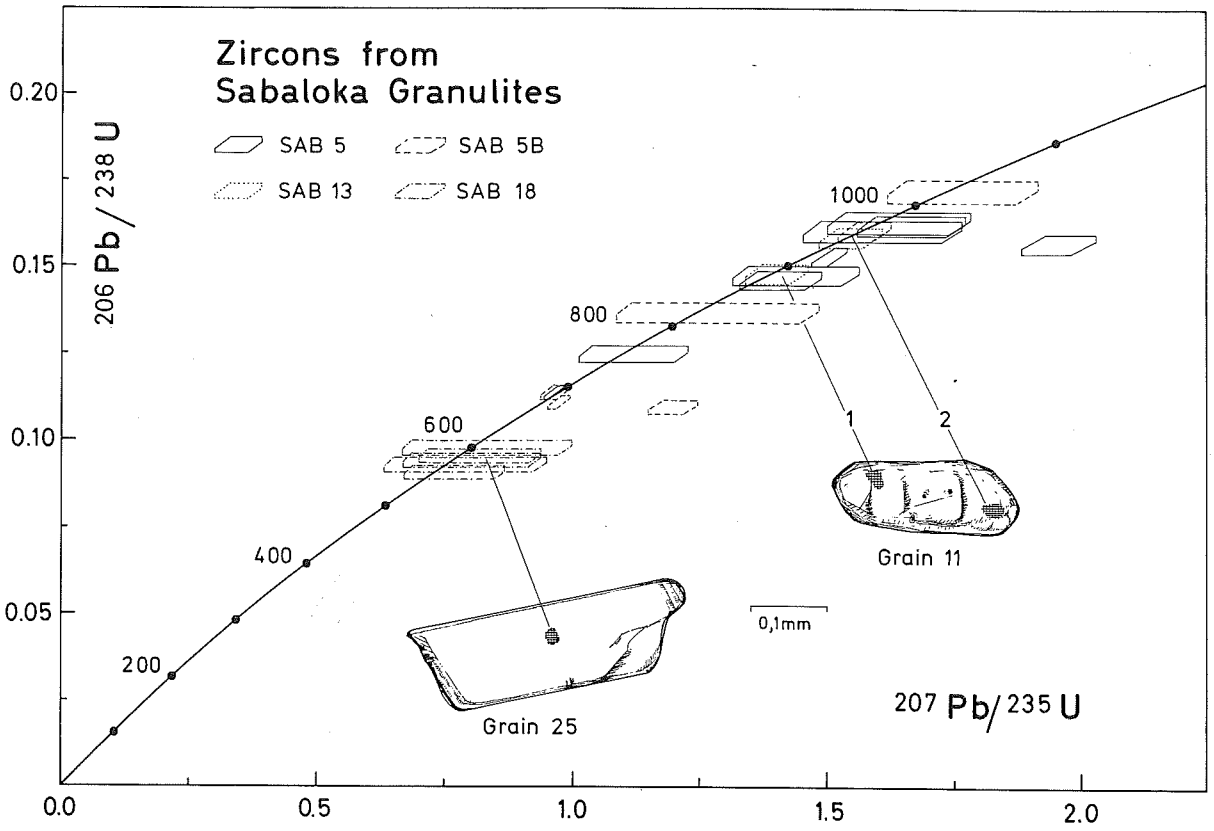

Fig. 6. Concordia diagram showing zircon data for granulites of sedimentary and igneous origin. Size of data boxes and insets as in Fig. 4.

$^{208}Pb/^{206}Pb$ ratio expected from the observed Th/U [16]. Details of the analytical technique are given in [16,18,19].

A total of 33 spots was measured during 7 mass scans for each spot analysis, and the results are presented in Table 3 and in the Concordia diagrams of Figs. 4 and 6. Data reduction follows Ludwig [20], and errors of ages quoted in the text are 2σ.

Rb/Sr ratios on whole-rock powder pellets were determined by XRF in Mainz following a method detailed elsewhere [21], and the precision is $\approx 1\%$ (2σ). Sr isotopic ratios were measured on unspiked samples, using the 12-inch radius, 60° sector field, solid-source mass spectrometer at the University of Texas at Dallas. Regression calculation is based on a combination of York [22] and statistical assessment after McIntyre et al. [23] and is detailed in [21]. The results are presented in Table 4 and in Figs. 7–9. All quoted errors are 2σ.

Sm-Nd analysis of a whole-rock sample of SAB 5 followed procedures outlined in [24] and was performed on a multi-collector Finnigan-Mat 261 mass spectrometer in the Max-Planck-Institut für Chemie in Mainz. The result is shown in Table 5.

Zircons from sample SAB 5 are well rounded and provide compelling evidence for sedimentary transport (Fig. 3). Most grains are also clear and display little internal zoning, a feature often found in granulitic zircons. Cores with dark inclusions, rimmed by clear, unzoned overgrowth are ubiquitous. In selecting suitable grains for ion microprobe analysis dark, U-rich material as well as grains with many inclusions were avoided. The oldest grain is egg-shaped, clear, with faint igneous zonation, and 3 spots define a chord with a lower intercept significantly above zero (Fig. 4). The $^{207}Pb/^{206}Pb$ ages of 2521–2624 Ma are thus *minimum* ages, and grain 1 may have a true crystallization age of about 2650 Ma.

Two spots were analyzed on grain 5, and these have widely varying isotopic ratios (Table 3, Fig. 4) that can be fitted to a chord intersecting concordia at 2006 ± 6 and 627 ± 11 Ma respectively. If the analyses of grains 3 and 6 are added to this array, the ages become 2000 ± 27 Ma and 631 ± 84

TABLE 4

Rb-Sr data and rock types for granulites, migmatites and granite from the Sabaloka area

Sample No.	Rock type	Metamorphic grade	Rb (ppm)	Sr (ppm)	Rb/Sr	$^{87}Rb/^{86}Sr$	$^{87}Sr/^{86}Sr$ [a]
SAB 5	garnet-cordierite-gneiss (mafic band)	granulite	128	63.9	1.99	5.8085	0.78447 ± 14
SAB 5B	garnet-cordierite gneiss (felsic band)	granulite	136	110	1.23	3.5690	0.76185 ± 10
SAB 13	garnet-cordierite-spinel -biotite-sillimanite gneiss (pelitic gneiss)	granulite	31.6	137	0.230	0.6678	0.73181 ± 13
SAB 1	diopside-plagioclase gneiss	granulite	0.20	292	0.0007	0.0020	0.70418 ± 17
SAB 12	diopside-garnet-plagioclase-scapolite gneiss	granulite	15.6	303	0.0511	0.1478	0.70609 ± 6
SAB 15	biotite-two pyroxene-hornblende-biotite gneiss	granulite	107	587	0.181	0.5237	0.70985 ± 12
SAB 16	plagioclase-diopside-hornblende gneiss	granulite	12.8	433	0.030	0.0859	0.70543 ± 7
SAB 18	plagioclase-quartz-two pyroxene-biotite-hornblende gneiss (enderbite)	granulite	73.7	596	0.124	0.3576	0.70785 ± 6
SAB 24	diopside-plagioclase-garnet-sphene gneiss	granulite	14.7	345	0.0426	0.1232	0.70545 ± 8
SAB 26	diopside-plagioclase-scapolite gneiss	granulite	7.1	187	0.0380	0.1099	0.70570 ± 8
SAB 27	diopside-scapolite-plagioclase gneiss	granulite	14.3	232	0.0617	0.1784	0.70652 ± 7
SAB 8	biotite-hornblende gneiss (paleosome in migmatite)	migmatite	131	319	0.409	1.1847	0.71608 ± 11
SAB 10	leucocratic garnet-biotite gneiss	migmatite	186	211	0.880	1.5243	0.72633 ± 7
SAB 17	quartz-microcline-plagioclase-biotite gneiss (paleosome in migmatite)	migmatite	156	174	0.890	2.5900	0.73394 ± 6
SAB 19	hornblende gneiss	migmatite	114	361	0.316	0.9195	0.71382 ± 8
SAB 20	quartz-microcline-plagioclase-biotite gneiss (paleosome in migmatite)	migmatite	166	314	0.526	1.5243	0.72123 ± 8
SAB 21	quartz-microcline-plagioclase-biotite-hornblende gneiss	migmatite	328	52.6	6.21	18.0814	0.85430 ± 9 [b] 0.85434 ± 7 [b]
SAB 42	very coarse porphyritic granite	Banjadeed granite	179	215	0.833	2.4144	0.72850 ± 8
SAB 43	very coarse porphyritic granite		182	212	0.859	2.4914	0.72947 ± 7
SAB 44	migmatitic patch in porphyritic granite		176	397	0.443	1.2840	0.71997 ± 10
SAB 45	very coarse porphyritic granite		246	291	0.843	2.4447	0.72900 ± 8

[a] Mean $^{87}Sr/^{86}Sr$ for E&A $SrCO_3 = 0.70792$. All data normalized to E&A $SrCO_3 = 0.70800$. Sr blanks < 3 ng.
[b] Separate dissolutions. Rb/Sr based on net peak intensity ratios [21], not on element concentrations.

Ma respectively. These data show that the lower intercept is significant, as in grain 1, and may indicate a severe Pb-loss event at Sabaloka towards the end of the Precambrian.

All other grains provide virtually concordant ages between 663 Ma and 1065 Ma (Fig. 4). Grain 10 has the highest U concentration of all zircons in sample SAB 5, and its morphology and age suggest metamorphic growth at 663 ± 25 Ma ago; it may thus reflect the Pb-loss event shown by the

pattern above. In summary, SAB 5 contains detrital zircons that range in age between 792 ± 195 Ma and about 2650 Ma and also indicate significant Pb loss and new zircon growth at about 665 Ma ago.

The whole-rock Sm-Nd isotopic systematics support the ancient nature of the sedimentary source terrain for sample SAB 5. Assuming a depositional age of 870 Ma for the Sabaloka metasediments, as seems realistic from the zircon ages, $\epsilon_{Nd}(T)$ is −3.7 while the respective Nd model ages are $T_{CHUR} = 1.26$ Ga and $T_{DM} = 1.70$ Ga (DM after [25]). These are *mean* crustal residence ages for the sedimentary source region, assuming that no Sm/Nd fractionation occurred during the crustal history, and compare well with the mean age for the detrital zircons.

Sample SAB 5B is also of sedimentary origin, but its zircons are less rounded and are much larger than those of SAB 5. Spectacular zoning is shown in long, prismatic grains of igneous origin that occur together with smaller, rounded and clear grains. Grain 14 has a core (14-1) and rim (14-2) with drastically different Th/U ratios, and the spots analyzed from these domains display a Pb-loss pattern similar to that of SAB 5 (Fig. 4). If the oldest three grains of SAB 5B are fitted to a chord the Concordia intercept ages are 2110 ± 160 and 520 ± 350 Ma respectively and are thus similar to those of sample SAB 5. Grains 13 and 18 are nearly concordant, have high U and have $^{207}Pb/^{206}Pb$ ages of 673 ± 88 Ma and 745 ± 45 Ma respectively. They are most likely reflecting new growth during the granulite event ≈ 720 Ma ago.

Only one round and unzoned grain could be analyzed from SAB 13 which is clearly of detrital origin. In view of the error in the $^{207}Pb/^{235}U$ ratio of the 2 spots measured it is not possible to decide whether Pb loss occurred recently or at the same time as in SAB 5 and 5B. The minimum age of this grain is therefore 901 ± 153 Ma, i.e. similar to the majority of zircons from the other two samples.

The zircons of SAB 18 are strikingly different from those described above and clearly reveal the igneous origin of their host rock. They are very clear, long, prismatic, unzoned and often display the typical conical ends that characterize magmatic growth (Fig. 5). The colourless, transparent appearance is also very typical of granulitic zircons, and any original zoning was probably obliterated during internal isotopic homogenization during slow cooling under granulite facies conditions. Five grains were analyzed but only provide imprecise ages due to their low content in radiogenic Pb (Table 3, Fig. 6). The $^{207}Pb/^{206}Pb$ dates vary between 627 and 809 Ma, and when the samples are regressed together, assuming recent Pb loss, the combined upper intercept age becomes 719 ± 81 Ma. In spite of this large error we consider this age to be significant since it is virtually identical to the time of new zircon growth in samples SAB 5 and 5B. We therefore conclude from the zircon data alone that the severe Pb-loss event at about 663–720 Ma and the igneous crystallization age of ≈ 720 Ma in sample SAB 18 reflect granulite metamorphism at Sabaloka in Pan-African times.

Rb-Sr whole-rock data points for the granulites are aligned along two distinct and different regression lines. The first line is defined by three samples of metasediments for which we discussed the zircon data above (SAB 5, 5B and 13) and yields an isochron (MSWD = 0.4) age of 721 ± 12 Ma (Fig. 7). The initial $^{87}Sr/^{86}Sr$ ratio (I_{Sr}) is 0.7249 ± 2, a value strongly suggesting crustal derivation of these rocks as already concluded from the geochemical data, the Nd model age and the zircon ages. We suggest that these sediments had virtually uniform $^{87}Sr/^{86}Sr$ ratios when they first equilibrated, perhaps during diagenesis, and we interpret the above age as reflecting the time of isotopic re-equilibration during an intense dehydration event that finally led to the dry granulites now sampled. The above Rb-Sr age is compatible with the Pb-loss event inferred from the zircon data and is virtually identical to the mean age of newly grown zircons in sample SAB 5B.

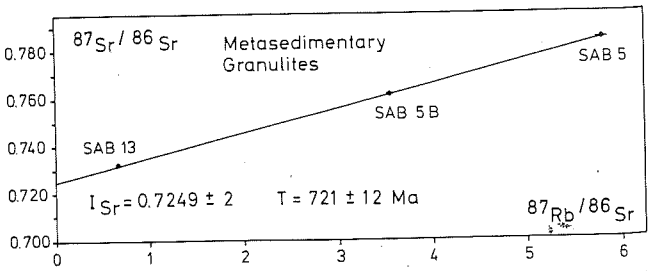

Fig. 7. Rb-Sr diagram for samples of Sabaloka granulites of sedimentary origin.

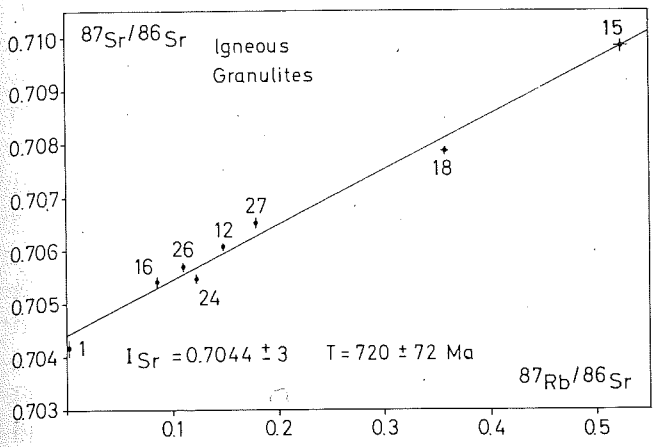

Fig. 8. Rb-Sr diagram for Sabaloka granulites of igneous derivation.

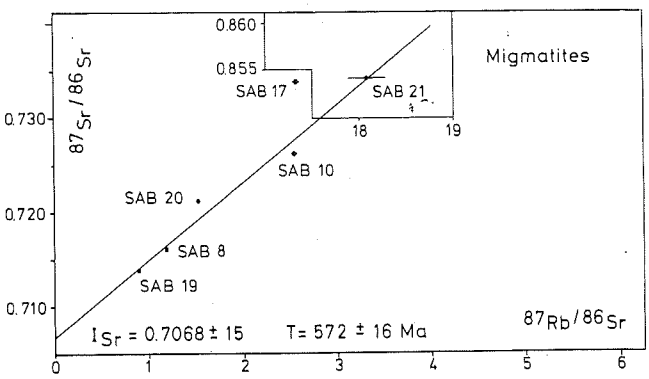

Fig. 9. Rb-Sr diagram showing isotopic data for Sabaloka migmatites.

The remaining granulites scatter about an errorchron (MSWD = 22.6) that corresponds to a Rb-Sr age of 696 ± 94 Ma (Fig. 8). This scatter most likely reflects incomplete homogenization during the prograde granulite event *or* isotopic disturbance during later retrogression. Statistical treatment of the data favours a McIntyre et al. [23] model 3 solution with an age of 720 ± 72 Ma and $I_{Sr} = 0.7044 \pm 3$. Although the error is reduced if the samples are plotted in two separate groups according to their geographic location (5 samples northwest of the railway line yield an isochron (MSWD = 2.1) age of 705 ± 38 Ma, $I_{Sr} = 0.7046 \pm 1$; 3 samples southeast of the railway line define an isochron (MSWD = 0.1) age of 720 ± 31 Ma, $I_{Sr} = 0.7042 \pm 1$), the age values do not change significantly and overlap within their errors, and we are not certain whether such separation is geologically justified. Thus, we suggest that the errorchron age of 696 ± 94 Ma is geologically meaningful within the error, particularly in view of its agreement with the zircon data and the metamorphic age for the metasediments. There is also evidence for igneous events of this age from the Bayuda Desert north of Sabaloka [9] and from the accretionary arc terranes of the Nubian shield to the east and northeast (see summaries in [8,26]).

The rocks defining the linear array with low I_{Sr} have a typical igneous mineralogy [5], and it was suggested from the geochemical data that the Ca-rich enderbitic rocks could have been anorthosites. Some samples are remarkably depleted in Rb; particularly in comparison with the lower-grade neighbouring migmatitic gneisses. We therefore suggest that the above age reflects the time of incomplete isotopic re-equilibration during a prograde metamorphic event that culminated in granulite genesis. Significant isotopic exchange during equilibration between the metasedimentary granulites with high initial I_{Sr} and the above igneous granulites with low I_{Sr} did not take place at scales represented by the sample distribution, in line with previous results from isotopic studies of granulite terrains [27].

Six samples of migmatitic gneisses that are associated with the granulites display considerable scatter about a regression line (MSWD = 52.3) which indicates a significantly younger age than for the granulites. The data distribution again favours a McIntyre et al. [23] model 3 solution and suggests an age of 572 ± 16 Ma with $I_{Sr} = 0.7068 \pm 15$ (Fig. 9). In this case we consider the scatter to reflect open system behaviour of Rb and Sr during retrograde metamorphism postdating granulitization. We suggest that the granulites now sampled remained dry and their Rb-Sr system was

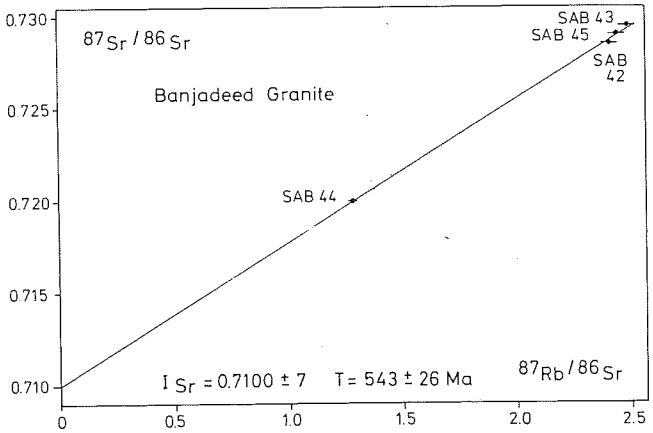

Fig. 10. Rb-Sr diagram for Banjadeed granite, Sabaloka.

TABLE 5

Sm-Nd data for granulite sample SAB 5

Sample	Nd (ppm)	Sm (ppm)	$^{147}Sm^{a}/^{144}Nd$	$^{143}Nd^{b}/^{144}Nd$	$\epsilon_{Nd}(T)$	Model age (Ga)	
						T_{CHUR}	T_{DM}
SAB 5	34.27	6.93	0.122308	0.512024 ± 15	−3.71	1.26	1.70

[a] Errors in isotopic ratios are 2σ (mean).

[b] Ratios are normalized to $^{146}Nd/^{144}Nd = 0.7219$. Value measured for the La Jolla Nd standard is $^{143}Nd/^{144}Nd = 0.511847 \pm 20$.

not significantly disturbed at that time while the biotite- and hornblende-bearing migmatites, in particular sample SAB 21, experienced resetting during the hydration event. The migmatites appear to be of igneous origin, and their elevated I_{Sr} suggests a crustal prehistory.

The peak of the hydration event is represented by anatexis in the migmatites and intrusion of the coarse, K-feldspar-rich, porphyritic Banjadeed granite. Four samples of this granite define an isochron (MSWD = 0.45) age of 543 ± 26 Ma and an I_{Sr} of 0.7100 ± 7 (Fig. 10), significantly lower than for the sedimentary granulites but still compatible with ultimate derivation of this granite from a source similar to the igneous granulites dated above. The granite age better approximates the peak of post-granulite metamorphism and anatexis than the migmatites, and a K-Ar age of 533 ± 20 Ma on gneiss south of Sabaloka [28] probably also records this event.

4. Discussion and conclusions

The first important conclusion from our data is that the Sabaloka granulites and gneisses are not Archaean in age. Instead they reflect Pan-African metamorphic events and were buried deep in the crust at that time while farther east, in the Red Sea Hills [8,29] and in Arabia [30,31] high-level volcanism and granitoid magmatism occurred. We note that a similar granulite age of 714^{+36}_{-49} Ma was reported for gneisses in the Mozambique belt of Tanzania previously regarded as Archaean [32].

Second, the isotopic data rule out an Archaean or early Proterozoic age for the precursors to the Sabaloka rocks. Although sample SAB 5 contains a detrital zircon indicating an Archaean source terrain, the sediment itself cannot have been older than about 870 Ma as documented by the appearance of abundant detrital zircons with ages from that time back to the mid-Proterozoic. Judging from the zircon data of samples SAB 5 and 5B, the predominant detrital input has an age between 870 and 1020 Ma, and we must assume that crust of this age was abundant in the vicinity of Sabaloka. Interestingly, a Sr model age calculation for the metasedimentary granulites, based on their mean Rb/Sr ratio and an assumed I_{Sr} of 0.706 as indicated for marine depositional environments of late Precambrian age [33] provided a figure of 1100 Ma which is similar to the above date and reflects the mean age of the detrital input into these sediments.

Third, our detrital zircon data provide the first direct evidence for sedimentary input from the Nile craton in this part of northeast Africa, and we suggest that this cratonic terrain is situated close to and west of Sabaloka. $\epsilon_{Nd}(T)$ values of −3.3 and −2.6 from quartzofeldspathic sediments of the eastern Bayuda Desert [34], i.e. directly north of Sabaloka, are compatible with our value of −3.7 for SAB 5, while rocks only slightly to the east yielded strongly positive ϵ values of +3.1 and +7.5. In the Eastern Desert of Egypt detrital zircon ages between ≈1120 and ≈1870 Ma were reported [35,36] that also reflect sedimentary input from the ancient shield to the west, while detrital zircons from Recent sands at the mouth of the River Nile yielded scattered ages indicating a 1540 ± 200 Ma old source terrain [37]. We therefore define the boundary between the old African continent (Nile craton) and the juvenile Nubian shield broadly along the River Nile [38]. The sedimentary precursors of the Sabaloka granulites were probably continental margin deposits that herald the beginning of the Pan-African episode of deposition, accretion and orogeny.

The relationship between crustal evolution at Sabaloka and that in the accretionary terranes farther east remains equivocal. One possible model

is that arc accretion in the east led to the collapse of the passive margin of the Nile craton, and that considerable horizontal shortening as has now been documented in the southern Eastern Desert of Egypt [8] and that is also evident from early, pre-metamorphic recumbent isoclinal folding in the Sabaloka granulites, resulted in crustal interstacking and thickening. This process finally brought the Sabaloka sediments to lower crustal levels where the increased heat flow that generated the enormous magmatic province of the Nubian shield converted them to granulites.

Finally, our data suggest that the East African Mozambique belt with similar high-grade gneiss assemblages and isotopic ages [32,39] extends from Tanzania, Kenya and northeast Uganda through the southern Sudan and western Ethiopia into the region of the River Nile. The gneisses studied here may represent the infrastructure of the ancient African continental margin.

An apparent lack of Pan-African detrital zircons in Recent Nile sands and other sediments in northern Africa led to the suggestion that the Pan-African mobile belts were not of collisional origin since they should have been elevated considerably during this process and shed their zircons into adjacent platform sediments [37]. We do not agree with this interpretation since the generation of granulites, coupled with intense horizontal shortening, is compelling evidence for crustal thickening and uplift in NE Africa. We suggest, however, that most of the detritus of the rising mountain chain was transported eastward, towards the present Red Sea, and we recognize this material in detrital Pan-African zircons from sediments east of the River Nile [40].

Acknowledgements

The zircon work was undertaken with assistance of I.S. Williams while A. Kröner held a Visiting Fellowship of the Australian National University in Canberra. Fieldwork of A. Kröner was funded by the Deutsche Forschungsgemeinschaft for R.J. Stern by Jet Propulsion Laboratory and for A.S. Dawoud by the University of Khartoum. We thank J. Vail and R. Van Schmus for critical reviews of an earlier version of the manuscript.

References

1 J.R. Vail, Outline of the geochronology and tectonic units of the basement complex of northeast Africa, Proc. R. Soc. London, Ser. A 350, 127–141, 1976.
2 G. Rocci, Essai d'interpretation de mésures geochronologiques. La structure de l'Ouest africain, Sci. Terre 10, 461–479, 1965.
3 A. Kröner, Pan-African plate tectonics and its repercussions on the crust of northeast Africa, Geol. Rundsch. 68, 565–583, 1979.
4 I.G. Gass, Pan-African (Upper Proterozoic) plate tectonics of the Arabian-Nubian shield, in Precambrian Plate Tectonics. Kröner, A., ed., pp. 387–405, Elsevier, Amsterdam, 1981.
5 D.C. Almond, Precambrian events at Sabaloka, near Khartoum, and their significance in the chronology of the basement complex of northeast Africa, Precambrian Res. 13, 43–62, 1980.
6 J.R. Vail, Outline of geology and mineralization of the Nubian shield east of the Nile valley, Sudan, in: Evolution and Mineralization of the Arabian-Nubian Shield, 1, S.A. Tahoun, ed., pp. 97–107, Pergamon Press, Oxford, 1979.
7 J. Klerkx and S. Deutsch, Résultats préliminaires obtenus par la méthode Rb/Sr sur des formations précambriennes de la region d'Uweinat (Libye), Mus. R. Afr. Centr., Tervuren (Belg.), Dep. Geol. Min., Rapp. Ann. 1976, pp. 83–94, 1977.
8 A. Kröner, R. Greiling, T. Reischmann, I.M. Hussein, R.J. Stern, S. Dürr, J. Krüger and M. Zimmer, Pan-African crustal evolution in the Nubian segment of northeast Africa, Am. Geophys. Union, Geodyn. Ser. 17, 235–257, 1987.
9 A.C. Ries and R.M. Shackleton, Geochronology, geochemistry and tectonics of the NE Bayuda Desert, N. Sudan: implications for the western margin of the late Proterozoic fold belt of NE Africa, Precambrian Res. 30, 43–62, 1985.
10 A. Kröner, Precambrian mobile belts of southern and eastern Africa - ancient sutures or sites of ensialic mobility? A case for crustal evolution towards plate tectonics, Tectonophysics 40, 101–135, 1977.
11 A.S. Dawoud, Geological and geophysical study of the area southeast of Qerri Station, eastern Sabaloka, Sudan. M.Sc. Thesis, University of Khartoum, Khartoum, 1971 (unpublished).
12 A.S. Dawoud and A.A. Sadig, Structural and gravity evidence for an uplifted Pan-African granulite terrain in Sabaloka inlier, Sudan, Geol. Rundsch., submitted.
13 J.S. Myers, The Fiskenaesset Anorthosite Complex — a stratigraphic key to the tectonic evolution of the West Greenland gneiss complex 3000–2800 m.y. ago, Geol. Soc. Austr., Spec. Publ. 7, 351–360, 1981.
14 J.M. Barton Jr., R.E.P. Fripp, P. Horrocks and N. McLean, The geology, age and tectonic setting of the Messina Layered Intrusion, Limpopo mobile belt, southern Africa, Am. J. Sci. 279, 1108–1134, 1979.
15 W. Compston, I.S. Williams and S.W.J. Clement, U-Pb ages within single zircons using a sensitive high mass-resolution ion microprobe, Ann. Conf. Am. Soc. Mass Spectrom., pp. 593–595, 1982.

16 W. Compston, I.S. Williams and C. Meyer, U-Pb geochronology of zircons from lunar breccia 73217 using a sensitive high mass-resolution ion microprobe, J. Geophys. Res. 89(Suppl.), B525–B534, 1984.
17 G.L. Cummings and J.R. Richards, Ore lead isotope ratios in a continuously changing earth, Earth Planet. Sci. Lett. 28, 155–171, 1975.
18 I.S. Williams, W. Compston, L.P. Black, T.R. Ireland and J.J. Foster, Unsupported radiogenic Pb in zircon: a cause of anomalously high Pb-Pb, U-Pb and Th-Pb ages, Contrib. Mineral. Petrol. 88, 322–327, 1984.
19 P.D. Kinny, I.S. Williams, D.O. Froude, T.R. Ireland and W. Compston, Early Archaean zircon ages from orthogneisses and anorthosites at Mount Narryer, Western Australia, Precambrian Res., in press, 1987.
20 K.R. Ludwig, Calculation of uncertainties of U-Pb isotopic data, Earth Planet. Sci. Lett. 46, 210–220, 1980.
21 A. Kröner, Rb-Sr geochronology and tectonic evolution of the Pan-African Damara belt of Namibia, southwestern Africa, Am. J. Sci. 282, 1471–1507, 1982.
22 D. York, Least-squares fitting of a straight line with correlated errors, Earth Planet. Sci. Lett. 5, 320–324, 1969.
23 G.A. McIntyre, C. Brooks, W. Compston and W. Turek, The statistical assessment of R-Sr isochrons, J. Geophys. Res. 71, 5459–5468, 1966.
24 W.M. White and J. Patchett, Hf-Nd-Sr isotopes and incompatible element abundances in island arcs: implication for magma origin and crust-mantle evolution, Earth Planet. Sci. Lett. 67, 167–185, 1984.
25 D.J. DePaolo, Neodymium isotopes in the Colorado Front Range and crust-mantle evolution in the Proterozoic, Nature 291, 193–196, 1981.
26 R.J. Stern and C.E. Hedge, Geochronologic and isotopic constraints on late Precambrian crustal evolution in the Eastern Desert of Egypt, Am. J. Sci. 285, 97–127, 1985.
27 S. Moorbath, Origin of granulites, Nature 312, 290, 1984.
28 J.R. Vail and D.C. Rex, Potassium-argon age measurements on pre-Nubian basement complex rocks from Sudan, Proc. Geol. Soc. London 1664, 205–214, 1971.
29 J.R. Vail, Pan-African crustal accretion in north-east Africa, J. Afr. Earth Sci. 1, 285–294, 1983.
30 R.J. Fleck, W.R. Greenwood, D.G. Hadley, R.E. Anderson and D.L. Schmidt, Rubidium-strontium geochronology and plate tectonic evolution of the southern part of the Arabian shield, U.S. Geol. Surv. Prof. Pap. 1131, 38 pp., 1980.
31 M.J. Roobol, C.R. Ramsay, N.J. Jackson and D.P.F. Darbyshire, Late Proterozoic lavas of the central Arabian shield—evolution of an ancient volcanic arc system, J. Geol. Soc. London 140, 185–202, 1983.
32 M.A.H. Maboko, N.A.I.M. Boelrijk, H.N.A. Priem and A.E.Th. Verdurmen, Zircon U-Pb and biotite Rb-Sr dating of the Wami River granulites, eastern granulites, Tanzania: evidence for approximately 715 Ma old granulite-facies metamorphism and final Pan-African cooling approximately 475 Ma ago, Precambrian Res. 30, 361–378, 1985.
33 J. Veizer and W. Compston, $^{87}Sr/^{86}Sr$ in Precambrian carbonates as an index of crustal evolution, Geochim. Cosmochim. Acta 40, 905–914, 1976.
34 N.B.W. Harris, C.J. Hawkesworth and A.C. Ries, Crustal evolution in northeast and east Africa from model Nd ages, Nature 309, 773–776, 1984.
35 T.H. Dixon, Age and chemical characteristics of some pre-Pan-African rocks in the Egyptian shield, Precambrian Res. 14, 119–133, 1981.
36 A.A. Abdel-Monem and P.M. Hurley, U-Pb dating of zircons from psammitic gneisses, Wadi Abu Rusheid-Wadi Sikait area, Egypt, Inst. Appl. Geol., Univ. Jeddah, Bull. 3(2), 45–55, 1979.
37 H.E. Gaudette und P.M. Hurley, Where were the Pan-African mountains? No evidence of 500 m.y. detrital zircons, Tectonophysics 54, 211–230, 1979.
38 T. Reischmann, Geologie und Genese spätproterozoischer Vulkanite der Red Sea Hills, Sudan, 202 pp., Ph.D. Thesis, University of Mainz, Mainz, 1986 (unpublished).
39 J.J.M.M.M. Coolen, H.N.A. Priem, A.E.Th. Verdurmen and R.A. Verschure, Possible zircon U-Pb evidence for Pan-African granulite-facies metamorphism in the Mozambique belt of southern Tanzania, Precambrian Res. 17, 31–40, 1982.
40 H.-J. Wust, W. Todt and A. Kröner, Conventional and single grain zircon ages for metasediments and granite clasts from the Eastern Desert of Egypt: evidence for active continental margin evolution in Pan-African times, Terra Cognita 7, 333–334.